Electronic Supplementary Information

An unprecedented 3D/3D hetero-interpenetrated MOF built from two different nodes, chemical composition, and topology of networks

Heng Xu,[1] Weiwei Bao,[1] Yan Xu,[1] Xiaolan Liu,[1] Xuan Shen[1], Dunru Zhu[1,2,*]

[1]*State Key Laboratory of Materials-Oriented Chemical Engineering, College of Chemistry and Chemical Engineering, Nanjing University of Technology, Nanjing 210009, P.R. China*
E-mail: zhudr@njut.edu.cn
[2]*State Key Laboratory of Coordination Chemistry, Nanjing University, Nanjing 210093, P.R. China*

Experimental Section

I. General remarks. All chemicals were of analytical grade and used as received. Elemental analyses (C, H, N) were carried out with a Thermo Finnigan Flash 1112A elemental analyzer. FT-IR spectrum was recorded on a Nicolet 380 FT-IR instrument (KBr discs) in the 4,000–400 cm^{-1} region. Thermogravimetric analysis (TGA) was performed on a NETZSCH STA 449C thermal analyzer under nitrogen atmosphere at a scan rate of 10 °C/min. Powder X-ray diffraction patterns (PXRD) were measured using a Brüker AXS D8 Advance powder diffractometer at 40 kV, 40 mA for Cu K_α (λ = 1.5406 Å), with a scan speed of 0.2 s/step and a step size of 0.02°.

II. Synthesis.

Synthesis of ligand 2,2'-dimethoxy-biphenyl-4,4'-dicarboxylic acid (H_2L): The ligand H_2L was synthesized by a method reported in ref. (1) (Scheme S1).

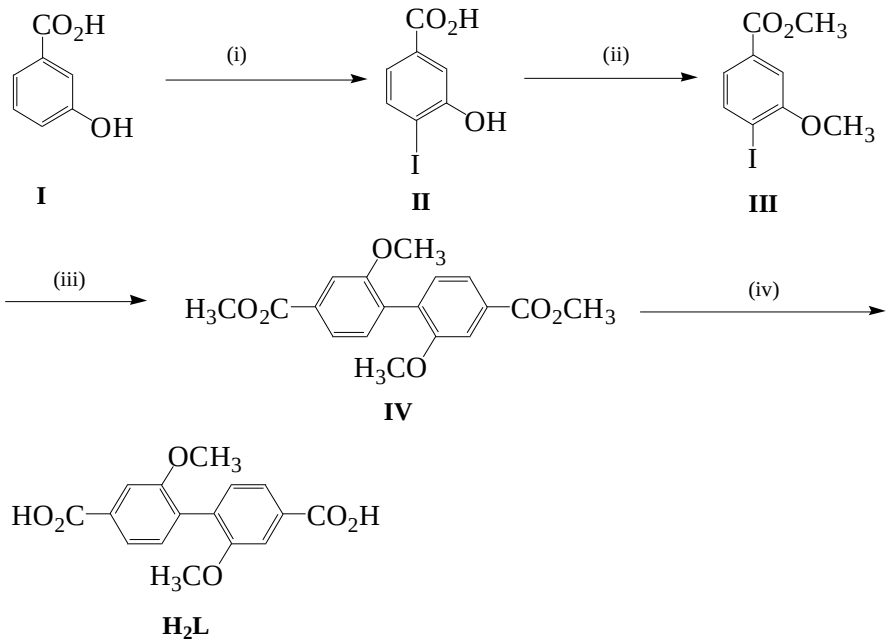

Scheme S1. The synthetic route of 2,2'-dimethoxy-biphenyl-4,4'-dicarboxylic acid (H_2L): (i) concentrated aqueous ammonia, KI, I_2, H_2O, (ii) dimethyl sulfate, K_2CO_3, acetone, (iii) activated copper powder, 210-220 °C, (iv) a) KOH, methanol, reflux, 1h; b) HCl.

Synthesis of $(Me_2NH_2)_6[Cd_3L_4]_2[CdL_2]\cdot 18H_2O\cdot 7Me_2NH\cdot 5DMF$ (1): A mixture of $Cd(NO_3)_2\cdot 4H_2O$ (0.0308 g, 0.1 mmol), H_2L (0.0302 g, 0.1 mmol), DMF(2 mL) and water (0.1 mL) was sealed in a 25 mL Teflon-lined stainless steel vessel and heated at 120 °C for 48 hours. Colourless octahedron-shaped crystals of **1** were collected, washed with DMF and dried in air. Yield of **1**: 0.046 g, 91% based on H_2L. Elemental analysis calcd (%) for $C_{201}H_{288}Cd_7N_{18}O_{83}$: C 47.60, H 5.72, N 4.97; found C 47.53, H 5.91, N 5.13. FT-IR (KBr, cm^{-1}): $\tilde{\nu}$ = 3449 (b, s), 2963 (w), 1655 (m), 1589 (s), 1541 (s), 1407 (s), 1241 (s), 1122 (w), 1042 (s), 1005 (w), 807 (s), 771 (s).

The MOF **1** was insoluble in common organic solvents such as acetone, methanol, ethanol, dichloromethane, acetonitrile, chloroform, and DMF.

III. Crystal-structure determination.

Intensity data for MOF **1** was collected on a Bruker SMART APEX II CCD area-detector diffractometer using graphite-monochromated Mo K_α radiation. The structures were solved by direct methods and subsequent difference Fourier syntheses, and refined using the SHELXTL software package.[2] Except for the guest molecules, non-hydrogen atoms were refined with anisotropic displacement parameters, and the hydrogen atoms of the ligands were calculated and refined as riding modes. The numbers of solvent water, DMF and dimethylamine

molecules are estimated duo to their highly disordered presentation, in which partial occupancies were applied. The final formula of MOF **1** was assigned by elemental analysis, IR, TGA, and single-crystal X-ray crystallography. The crystal data and structure refinement of MOF **1** are summarized in Table S1. The selected bond lengths (Å) and angles (°) for MOF **1** are listed in Table S2. Crystallographic data for MOF **1** have been deposited with the Cambridge Crystallograhic Data Centre as supplementary publications CCDC-728873 (**1**). The data can be obtained free of charge from The Cambridge Crystallographic Data Centre via www.ccdc.cam.ac.uk/data_request/cif.

Table S1 Crystal data and structure refinement for **1**

MOF	**1**
Empirical formula	$C_{201}H_{288}N_{18}O_{83}Cd_7$
Formula weight	5071.39
Temperature (K)	291(2)
Wavelength (Å)	0.71073
Crystal size (mm^3)	0.13 × 0.13 × 0.12
Crystal system	Tetragonal
Space group	$I\bar{4}2d$
a (Å)	22.180(3)
b (Å)	22.180(3)
c (Å)	43.666(9)
V ($Å^3$)	21481(6)
Z	4
Density ($g \cdot cm^{-3}$)	1.324
F(000)	8712
Absorption coeff. (mm^{-1})	0.760
θ range (º)	1.84-26
h/k/l	-27,14/-27,25/-53,52
Reflections collected	57376
Independent reflections	10563 [R_{int} = 0.0666]
Observed reflections	9437
Data/restraints/parameters	10563/0/637
Goodness-of-fit on F^2	1.059
R, *wR* indices [$I > 2\sigma(I)$]	0.0514, 0.1225
R, *wR* indices (all data)	0.0588, 0.1262
Largest diff. peak and hole ($e \cdot Å^{-3}$)	0.665, -0.983

Table S2 Selected bond lengths (Å) and angles (°) for **1**

Bond lengths			
Cd(1)-O(3)^{ii}	2.261(4)	Cd(1)-O(10)^{i}	2.286(4)
Cd(1)-O(9)^{i}	2.383(4)	Cd(1)-O(7)	2.394(4)
Cd(1)-O(8)	2.407(3)	Cd(1)-O(2)	2.412(4)
Cd(1)-O(1)	2.482(4)	Cd(2)-O(4)^{iii}	2.167(3)
Cd(2)-O(2)	2.315(4)	Cd(2)-O(7)	2.315(4)
Cd(3)-O(14)	2.310(4)	Cd(3)-O(13)	2.527(4)
Bond angles			
O(3)^{ii}-Cd(1)-O(10)^{i}	106.77(14)	O(4)^{ii}-Cd(2)-O(4)^{iii}	174.55(18)
O(3)^{ii}-Cd(1)-O(9)^{i}	84.95(15)	O(4)^{ii}-Cd(2)-O(7)	87.03(14)
O(10)^{i}-Cd(1)-O(9)^{i}	54.94(14)	O(4)^{iii}-Cd(2)-O(7)	89.41(13)
O(3)^{ii}-Cd(1)-O(7)	94.32(14)	O(7)^{iv}-Cd(2)-O(7)	98.3(2)
O(10)^{i}-Cd(1)-O(7)	155.85(13)	O(4)^{ii}-Cd(2)-O(2)	92.68(13)
O(9)^{i}-Cd(1)-O(7)	117.31(13)	O(4)^{iii}-Cd(2)-O(2)	90.88(14)
O(3)^{ii}-Cd(1)-O(8)	137.02(14)	O(7)^{iv}-Cd(2)-O(2)	177.91(15)
O(10)^{i}-Cd(1)-O(8)	102.28(13)	O(7)-Cd(2)-O(2)	81.71(13)
O(9)^{i}-Cd(1)-O(8)	86.57(13)	O(2)^{iv}-Cd(2)-O(2)	98.40(19)
O(7)-Cd(1)-O(8)	53.59(12)	O(14)^{v}-Cd(3)-O(14)	102.35(8)
O(3)^{ii}-Cd(1)-O(2)	85.42(14)	O(14)-Cd(3)-O(14)^{vi}	124.90(18)
O(10)^{i}-Cd(1)-O(2)	114.48(13)	O(14)-Cd(3)-O(14)^{vii}	102.35(8)
O(9)^{i}-Cd(1)-O(2)	162.38(13)	O(14)-Cd(3)-O(13)^{v}	82.14(13)
O(7)-Cd(1)-O(2)	78.12(11)	O(14)-Cd(3)-O(13)^{vi}	83.72(14)
O(8)-Cd(1)-O(2)	110.42(13)	O(14)^{v}-Cd(3)-O(13)	148.97(13)
O(3)^{ii}-Cd(1)-O(1)	137.68(14)	O(14)-Cd(3)-O(13)	52.36(13)
O(10)^{i}-Cd(1)-O(1)	83.50(14)	O(14)^{vi}-Cd(3)-O(13)	83.72(14)
O(9)^{i}-Cd(1)-O(1)	130.22(14)	O(14)^{vii}-Cd(3)-O(13)	82.14(13)
O(7)-Cd(1)-O(1)	88.79(14)	O(13)^{v}-Cd(3)-O(13)	127.30(12)
O(8)-Cd(1)-O(1)	75.97(15)	O(13)^{vi}-Cd(3)-O(13)	77.8(2)
O(2)-Cd(1)-O(1)	53.96(13)		

Symmetry codes: i) *x* -1/2, *y*, 1/4+*z*; ii) *x* -1/2, 1+*y*, 1/4+*z*; iii) *x* -1/2, 1/2-*y*, 1/2-*z*; iv) 3/2-*x*, *y*, 3/4-*z*; v) *x*, 1-*y*, 1-*z*; vi) 1-*x*, 1-*y*, *z*; vii) 1-*x*, y, 1-*z*.

IV. ^{113}Cd NMR spectrum of 1. The solid state ^{l13}Cd NMR spectrum of **1** was obtained from 0.1221 g of the crystalline sample on the Bruker AM 400 NMR spectrometer operating at 88.745 MHz using CP-MAS techniques. The contact time was 3.5 ms, the delay time was 2 s, and the rotor speed was set at 14 kHz**.** Chemical shift was quoted relative to 0.1 mol L^{-1} $Cd(C1O_4)_2$ aqueous (D_2O) solution as a reference with positive chemical shift downfield. The spectrum of **1** is shown in Figure S1 and the three peaks at δ −24.6, −51.4, and −72.4 ppm, are assigned to the 6-, 7-, and 8-coordinated Cd^{2+} ions, respectively.[3]

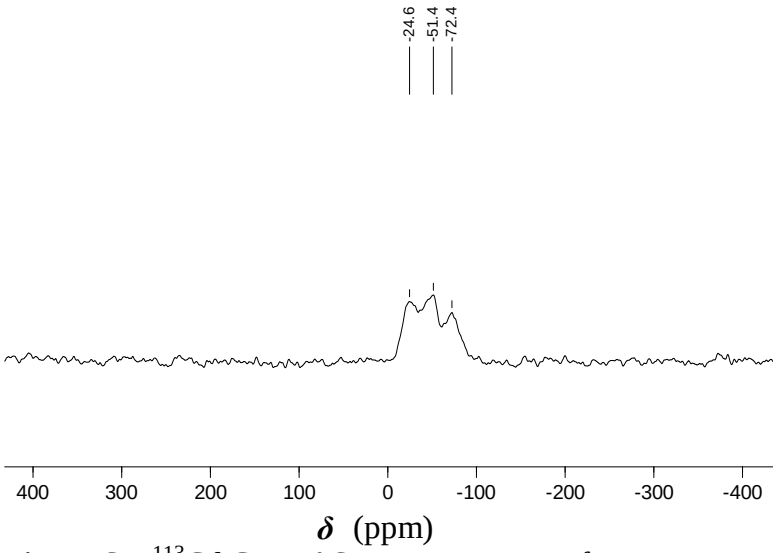

Figure S1. ^{113}Cd CP-MAS NMR spectrum of **1**.

V. Molecular Structures

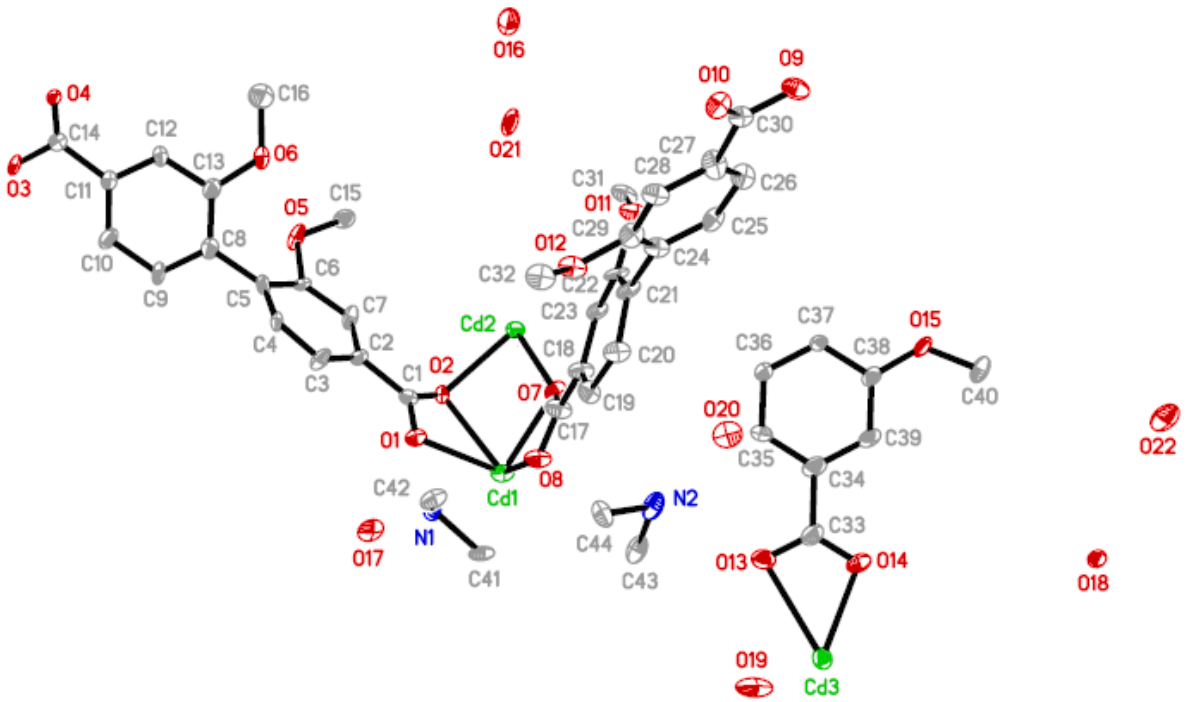

Figure S2. ORTEP drawing (at 30% probability) of the asymmetric unit for MOF **1** (All H atoms are omitted for clarity).

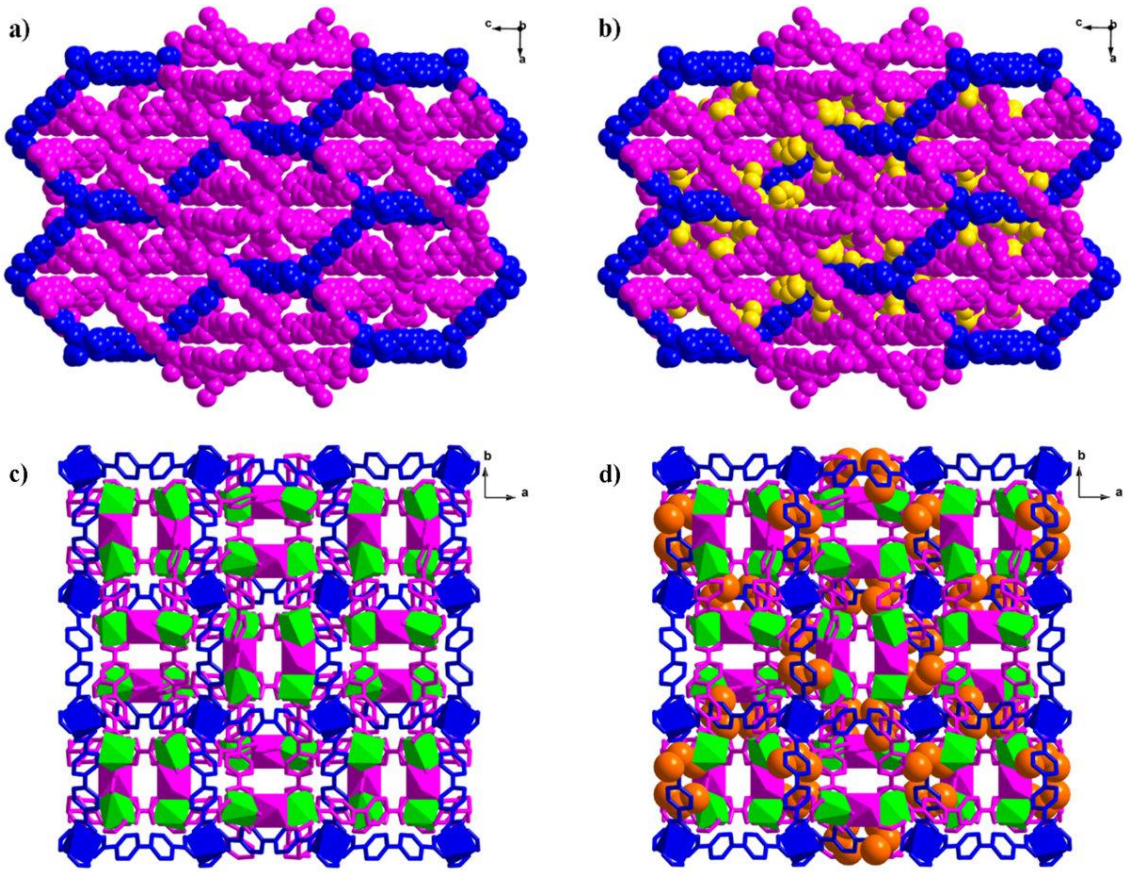

Figure S3. Two-fold 3D/3D hetero-interpenetrated networks in MOF **1** along *b* (a and b) and *c* axis (c and d). a) and b) represent without and with solvent molecules, respectively (The MeO groups, H atoms and $Me_2NH_2^+$ cations are omitted for clarity; red: 8-connected CsCl framework from linear $Cd_3(CO_2)_8$ cluster; blue: diamond network from $Cd(CO_2)_4$ unit; yellow: solvent molecules). c) and d) represent without and with $Me_2NH_2^+$ cations, respectively (The MeO groups, H atoms and solvent molecules are omitted for clarity; blue, green, red polyhedron shows 8-, 7-, 6-coordinated Cd^{2+}, respectively, orange: $Me_2NH_2^+$ cations).

VI. Coordination modes of the ligand:

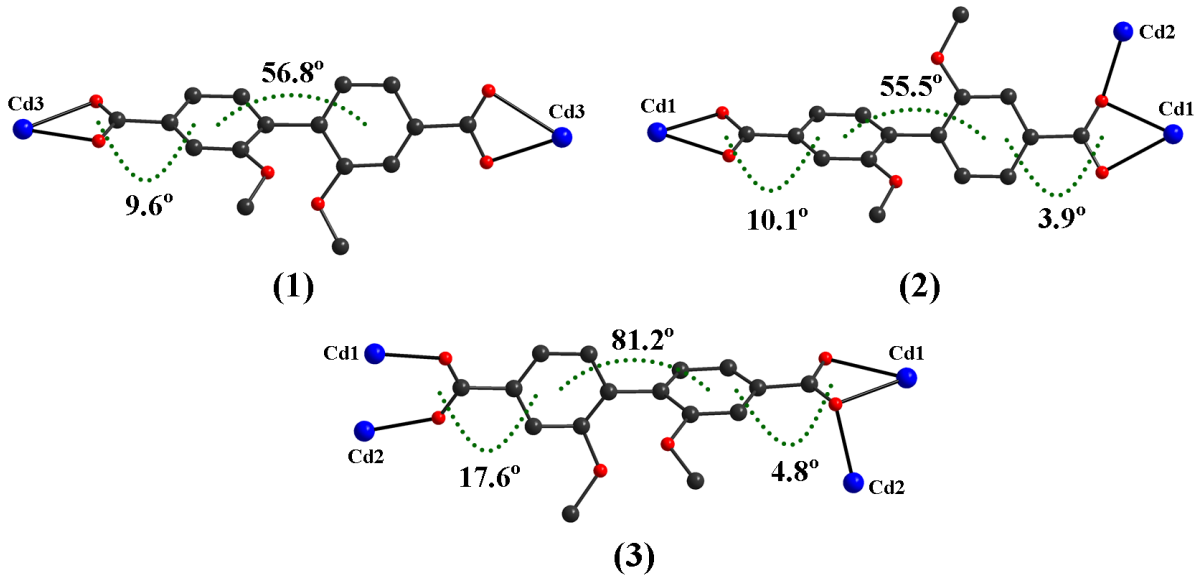

Scheme S3. Coordination modes and the dihedral angles of L in MOF **1**

VII. The FT-IR spectrum:

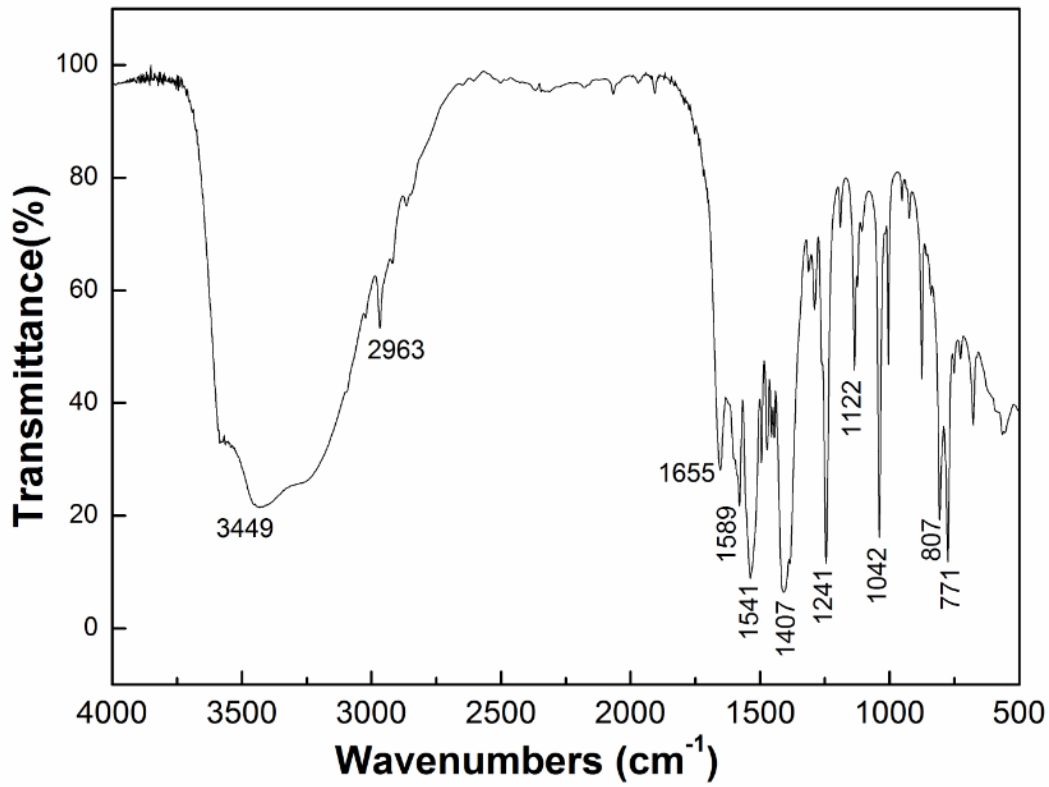

Figure S4. The FT-IR spectrum of MOF **1**.

VIII. The variable temperature PXRD patterns:

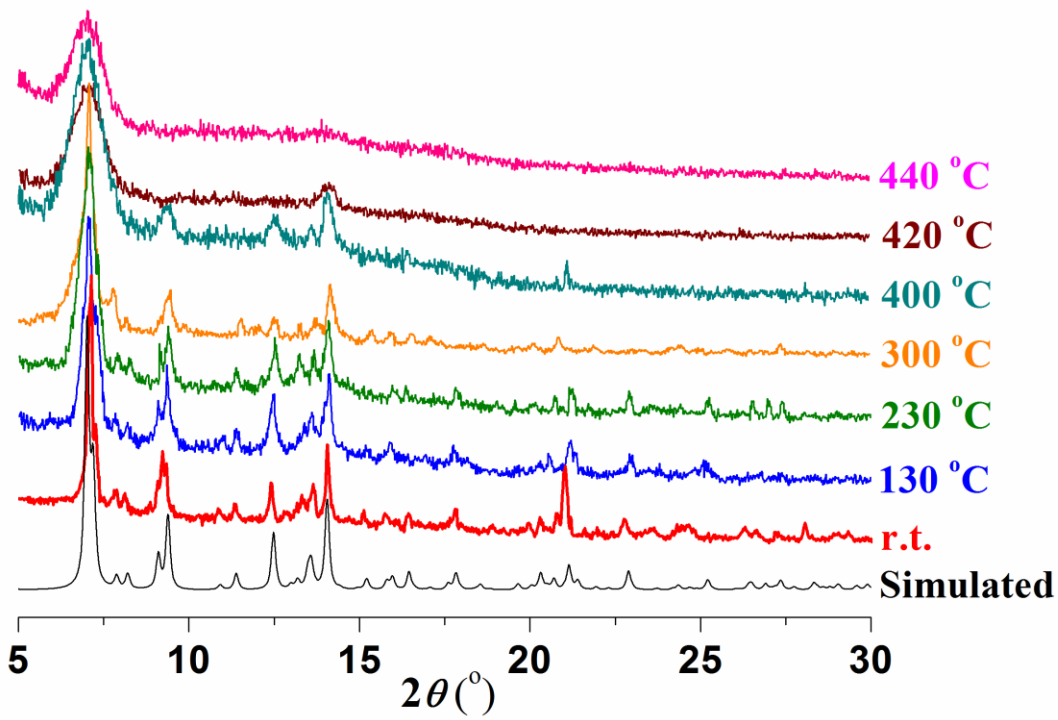

Figure S5. The variable temperature PXRD patterns of MOF **1**. The simulated pattern generated from single-crystal diffraction data.

IX. Thermogravimetric analysis:

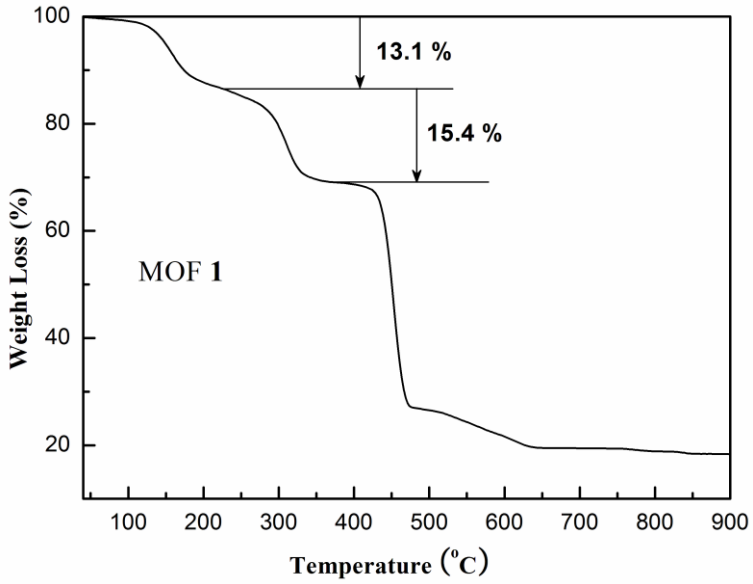

Figure S6. Thermogravimetric analysis curves of MOF **1**.

X. Nonlinear Optical Measurement. Second-order nonlinear optical effect for the powder samples of **1** was investigated by optical second-harmonic generation (SHG) at room temperature.[4] SHG intensity data were obtained by placing the powder sample in an intense fundamental beam from a Q-switched Nd: YAG laser with a wavelength 1064 nm. The output (λ = 532 nm) was filtered firstly to remove the multiplier and then displayed on an

oscilloscope. This procedure was repeated using a standard NLO material (microcrystalline urea), and the ratio of the second-harmonic intensity outputs was calculated. The observed SHG efficiency of **1** is *ca.* 0.8 times that of urea (Scheme S3).

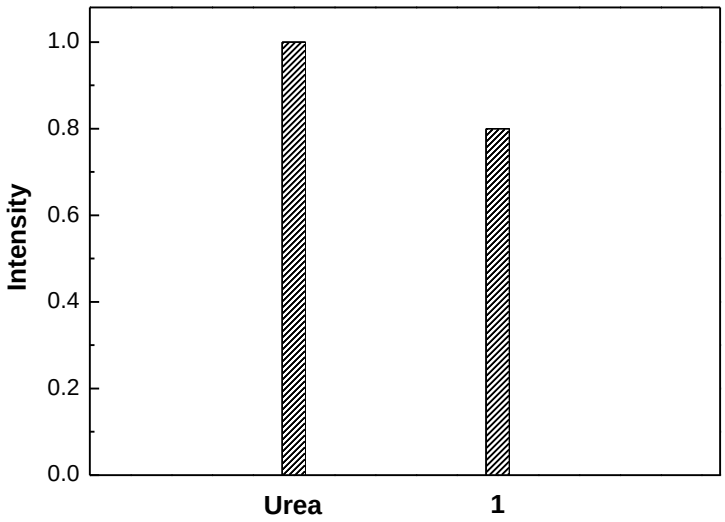

Scheme S3. SHG efficiency of **1** compared with urea.

References

(1) D.-R. Zhu, W.-W. Bao, X.-Z. Wang, X. Shen, Patent CN101362688A, 2009.

(2) G. M. Sheldrick, *Acta Crystallogr.* 2008, **A64**, 112.

(3) K. H. Chung, E. Hong, Y. Do, C. H. Moon, *J. Chem. Soc., Chem. Commun.* 1995, 2333.

(4) S. K. Kurtz and T. T. Perry, *J. Appl. Phys.*, 1968, **39**, 3798.